Metal–Organic Clusters Hot Paper

International Edition: DOI: 10.1002/anie.201501701
German Edition: DOI: 10.1002/ange.201501701

Controllable Scission and Seamless Stitching of Metal–Organic Clusters by STM Manipulation**

*Huihui Kong, Likun Wang, Qiang Sun, Chi Zhang, Qinggang Tan, and Wei Xu**

Abstract: *Scanning tunneling microscopy (STM) manipulation techniques have proven to be a powerful method for advanced nanofabrication of artificial molecular architectures on surfaces. With increasing complexity of the studied systems, STM manipulations are then extended to more complicated structural motifs. Previously, the dissociation and construction of various motifs have been achieved, but only in a single direction. In this report, the controllable scission and seamless stitching of metal–organic clusters have been successfully achieved through STM manipulations. The system presented here includes two sorts of hierarchical interactions where coordination bonds hold the metal–organic elementary motifs while hydrogen bonds among elementary motifs are directly involved in bond breakage and re-formation. The key to making this reversible switching successful is the hydrogen bonding, which is comparatively facile to be broken for controllable scission, and, on the other hand, the directional characteristic of hydrogen bonding makes precise stitching feasible.*

The direct identification of intermolecular interactions and the delicate tailoring of structural motifs with molecular precision on solid surfaces have recently attracted considerable interest because of the prospect for artificial design of functional molecular nanostructures and nanodevices. Scanning tunneling microscopy (STM), especially under ultrahigh vacuum (UHV) conditions, has proven to be a powerful method for the precise manipulation of single molecules to trigger various single-molecule behaviors, such as translation,[1–3] rotation,[3–9] flipping,[10] *cis–trans* isomerization,[11–13] tautomerization,[14–16] dehydrogenation,[17–19] and dehalogenation.[20] Not limited to single molecules, STM manipulations have also been extended to larger molecular structural motifs with great progress in the following aspects: 1) moving clusters,[21] chains,[22–25] and patches;[26] 2) dissociating dimers, clusters, and complexes by breaking hydrogen bonds,[27] coordination bonds,[28–30] and carbon–metal bonds,[31] respectively; 3) constructing structural motifs by forming new bonds ranging from hydrogen bonds,[32] coordination bonds,[30,33] to robust covalent bonds;[20,34,35] and 4) probing different hierarchical interactions[36] and identifying hydrogen-bonding configurations[27] and covalent bonding sites.[37] Most of the previous studies mentioned above mainly exhibited either the dissociation or construction of various structural motifs. However, to the best of our knowledge, the reversible switching of complicated structural motifs by controllable breakage and re-formation of certain bonds through STM manipulations has not been reported to date. It is therefore of great interest to explore the feasibility of utilizing STM manipulations to achieve controllable scission and precise stitching of complicated structural motifs in a comparatively facile manner, which may open a new avenue for the artificial fabrication of desired surface nanostructures with more complexity.

To achieve this goal, the strategy employed in this study entailed to first design a system that includes two sorts of hierarchical interactions. We chose a nucleobase, namely uracil (U; see Figure 1b), as a potential candidate to interact with Ni atoms.[38] From the interplay of STM imaging and lateral STM manipulations together with density functional theory (DFT) calculations, we show that 1) co-deposition of U molecules and Ni atoms on the Au(111) surface results in the formation of isolated triangular metal–organic coordination clusters. Subsequently, these triangular clusters can serve as the elementary motifs and be connected with another one or more through hydrogen bonds to self-assemble into parallelogrammic clusters or even more complicated higher-level structures. 2) Interestingly, lateral STM manipulations allow us to achieve the controllable scission of higher-level structures into their elementary motifs by breaking the hydrogen bonds while the coordination bonds holding the triangular clusters are kept unperturbed. 3) Moreover, the seamless stitching of elementary motifs into higher-level structures through re-formation of hydrogen bonds is also achieved. 4) Furthermore, the reversible switching of metal–organic motifs provides us with an effective way to modulate the electronic properties of the metal centers, which is confirmed by DFT calculations.

Co-deposition of U molecules and Ni atoms at a low surface coverage (ca. 0.05 monolayer (ML)) on a Au(111) surface held at 400 K led to the formation of triangular clusters discretely distributed on the surface (Figure 1a). Statistical analysis revealed that there are only two adsorption orientations (the included angle between the two orientations is 60°) for the triangular clusters. After further annealing the sample at 400 K for 15 minutes, we found that parallelogrammic clusters appeared and coexisted with the triangular clusters as shown in Figure 1b. The close-up STM images

[*] H. Kong, L. Wang, Q. Sun, C. Zhang, Dr. Q. Tan, Prof. Dr. W. Xu
Tongji-Aarhus Joint Research Center for Nanostructures and Functional Nanomaterials, College of Materials Science and Engineering, Tongji University
Caoan Road 4800, Shanghai 201804 (P. R. China)
E-mail: xuwei@tongji.edu.cn

[**] We acknowledge financial support from the National Natural Science Foundation of China (21103128, 21473123) and the Research Fund for the Doctoral Program of Higher Education of China (20120072110045).

Supporting information for this article is available on the WWW under http://dx.doi.org/10.1002/anie.201501701.

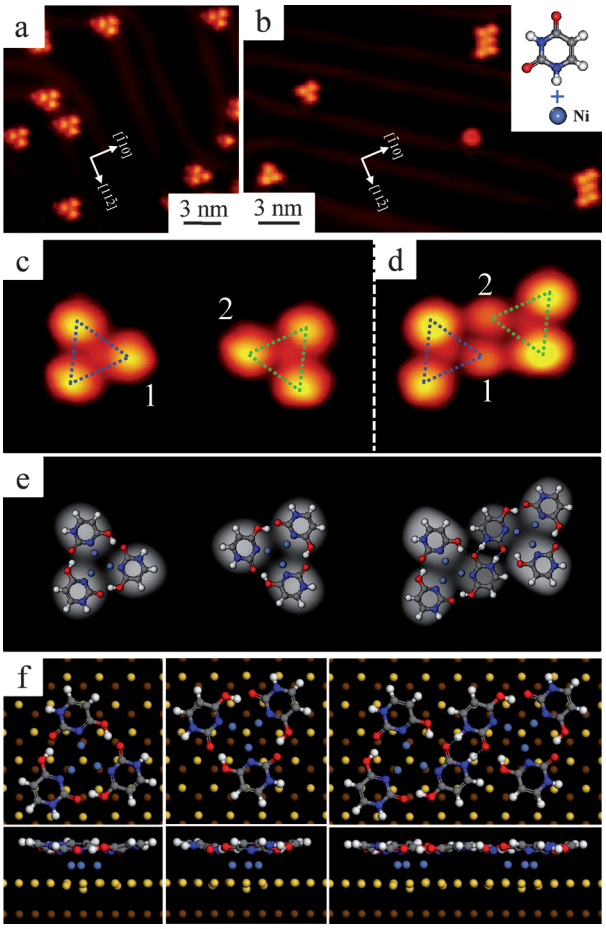

Figure 1. a, b) STM images showing the formation of triangular and parallelogrammic clusters on Au(111), respectively. c, d) Close-up STM images showing two triangular clusters with distinct orientations (indicated in blue and green) and a parallelogrammic cluster, respectively. e) Simulated STM images of triangular and parallelogrammic clusters superimposed with the DFT-optimized models on Au(111); the substrate is omitted for clarity. f) The corresponding top and side views of the models on Au(111). Scanning conditions: $I_t = 1.03$ nA, $V_t = 1.25$ V; STM image simulations at a bias voltage of 1.2 V.

(Figure 1c) reveal that the triangular clusters consist of three bright protrusions attributed to the U molecules, and in a special tip state, a central spot was also visible (Supporting Information, Figure S1), which should be related to the electronic states of the Ni atoms. The blue and green triangles drawn in Figure 1c represent two distinct orientations of the triangular clusters. The close-up STM image (Figure 1d) showed that the parallelogrammic cluster is composed of two triangular clusters with different orientations as intuitively depicted by the blue and green triangles. It is noticeable that the molecules 1 and 2 in the original triangular clusters (indicated in Figure 1c) become dim (with an apparent height difference of ca. 0.5 Å as determined by the line scan profiles shown in Figure S2d, e) when forming a parallelogrammic cluster (indicated in Figure 1d).

To unravel the atomic-scale structures of the triangular and parallelogrammic clusters, detailed DFT calculations that included the Au(111) substrate were performed. First, we built up structural models of the triangular clusters based on the canonical form of the U molecule; however, we identified that the most stable parallelogrammic model did not agree with the experimental configuration as illustrated in Figure S3. As it is known that the nucleobases can undergo tautomerization on surfaces,[39–41] we then re-built our models taking into account the non-canonical forms of the U molecule. After an extensive structural search and comparison with STM images, we identified the energetically favorable models of the triangular and parallelogrammic clusters, which were overlaid on the corresponding simulated STM images (Figure 1e); good agreements are achieved when comparing them with the experimental morphologies and dimensions. The optimized models showed that the triangular cluster was formed by three U molecules coordinating to three Ni atoms, and that the parallelogrammic cluster was formed by two homochiral triangular clusters linked together through double N–H···O hydrogen bonds. Interestingly, we found that the two dim molecules mentioned above are just the ones that are involved in the formation of hydrogen bonds. We thus believe that the change in apparent heights of molecules 1 and 2 (Figure 1c, d) should be attributed to the corresponding change in their molecular adsorption configurations upon hydrogen-bond formation.[27]

Furthermore, from the models of the triangular clusters, one would expect that such a cluster can be linked to another one (with the same chirality but a different orientation) from three distinct directions by the equivalent double N–H···O hydrogen bonds, which results in the formation of three kinds of parallelogrammic clusters. Experimentally, we indeed observed three different parallelogrammic clusters (Figure S4a–c), and the corresponding enantiomers were also detected (Figure S4d–f). We then expected that the formation of more complicated higher-level structures should also be possible. By increasing the surface coverage (up to ca. 0.2 ML), we obtained various self-assembled clusters (Figure 2a). The close-up STM images together with the relaxed gas-phase models shown in Figure 2b–i show that all of the higher-level structures consist of different numbers of homochiral triangular clusters linked through the same double N–H···O hydrogen bonds as in the parallelogrammic cluster. Interestingly, the rule that the molecules become dim when participating in the formation of hydrogen bonds is also applicable here (the translucent ellipse in each model indicates the hydrogen-bonding sites).

In the next step, we explored the feasibility of utilizing STM manipulations to perturb the hierarchically self-assembled higher-level clusters. As shown in Figure 3a–d, lateral STM manipulations were performed on a parallelogrammic cluster and a more complicated cluster (consisting of three triangular clusters). Interestingly, controllable scission of the higher-level clusters into their elementary triangular clusters was achieved by breaking the N–H···O hydrogen bonds. During this process, the metal–organic triangular clusters were kept intact and moved on the surface as a whole. In this sense, the applied STM manipulations successfully distinguished the hierarchical interactions (i.e., hydrogen bonding and coordination bonding) within the higher-level clusters, and moreover selectively broke the hydrogen bonds. Also, the

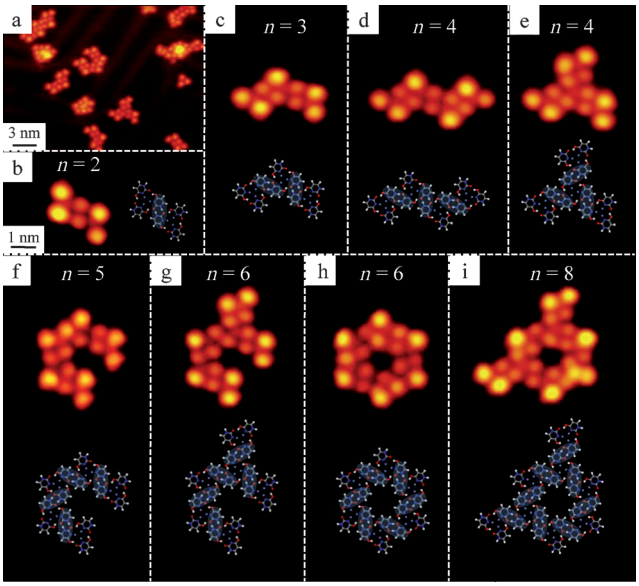

Figure 2. a) STM image showing the formation of higher-level clusters by increasing the surface coverage and annealing at 400 K for 15 minutes. b–i) Close-up STM images and the corresponding DFT-relaxed gas-phase models of various higher-level clusters consisting of different numbers of triangular clusters. Scanning conditions: $I_t = 1.03$ nA, $V_t = 1.25$ V.

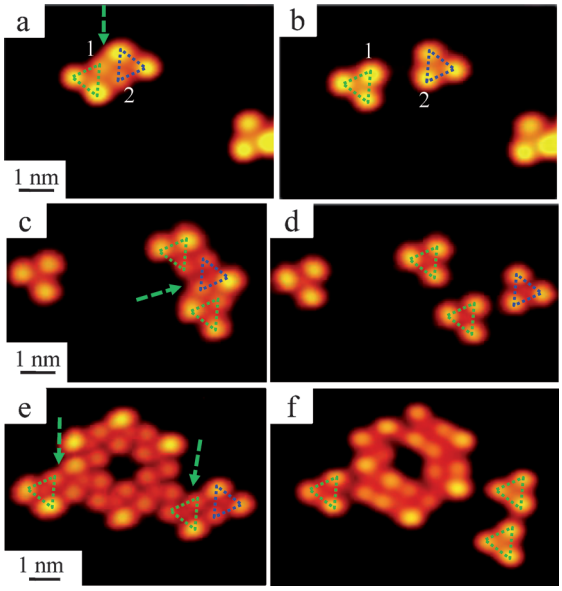

Figure 3. a, b) and c, d) Lateral STM manipulations demonstrating the controllable scission of higher-level clusters into isolated triangular clusters. e, f) STM manipulations were used to delicately trim the higher-level cluster. The green arrows indicate the directions of the STM manipulations.

two dim molecules 1 and 2 (indicated in Figure 3a) recovered their original appearance (i.e., became bright as indicated in Figure 3b) after the parallelogrammic cluster had been cut into two isolated triangular clusters, which implies that the molecular adsorption configuration relaxes back when the hydrogen bonds are broken. Furthermore, by employing such STM manipulations, we were able to delicately trim a more complicated cluster into an artificial hexagonal pattern as shown in Figure 3e, f. We were not only able to translate the triangular cluster, but also to rotate it on the surface (as indicated by the blue and green triangles in Figure 3f). Finally, a series of consecutive STM manipulations on a variety of larger clusters were also performed (Figure S5).

Fabrication of artificial molecular nanostructures requires reversible switching of structural motifs; therefore, we performed further STM manipulations in an attempt to achieve precise stitching of elementary motifs into higher-level structures through re-formation of hydrogen bonds. As illustrated in Figure 4a–d, a series of STM manipulations allowed us to achieve a reversible process of breaking a parallelogrammic cluster into two triangular ones and, more importantly, precise stitching them back into the parallelogrammic cluster. The key to making this process successful is the hydrogen bonding, which is comparatively facile to be broken to achieve controllable scission, and on the other hand, the directional characteristic makes seamless stitching feasible. Furthermore, as previously reported,[17,28,42] STM manipulations have been employed on organic molecules to either change the two-dimensional self-assembly or break a peripheral C–H bond of a single molecule, and even to directly perturb single coordination bonds to modulate the electronic properties of the single metal centers. Inspired by these reports, we speculated that the transformation from an isolated elementary metal–organic motif into a higher-level one and vice versa might have an influence on the electronic properties of the metal centers as well. We then performed further PDOS calculations on the different d orbitals of the Ni trimer in an isolated triangular cluster and in the same triangle within a parallelogrammic cluster (Figure 4e, f, respectively). It is noteworthy that 1) the peaks of the d_{xz} and d_{yz} orbitals of the Ni trimer in an isolated triangular cluster overlap with each other (Figure 4e), whereas they are separated in the same triangle within a parallelogrammic cluster (Figure 4f). 2) As indicated by the purple arrows, the main peak of the d_{z^2} orbital moves toward the Fermi energy (the d_{total} orbital shows the same tendency) when comparing the isolated triangular cluster (Figure 4e) to that within a parallelogrammic cluster (Figure 4f). Consequently, the reversible scission and stitching of metal–organic motifs by STM manipulations provides an alternative way to modulate the electronic properties of the metal centers.

In conclusion, by the combination of high-resolution STM imaging/lateral manipulation with DFT calculations, we have demonstrated the hierarchical self-assembly of metal–organic clusters where coordination bonds determine the formation of the elementary structural motifs in the first place, and hydrogen bonds direct the subsequent formation of higher-level structures. STM manipulations allowed us to selectively perturb the relatively weak hydrogen bonding and achieve controllable scission and seamless stitching of metal–organic clusters on the surface and moreover, to modulate the corresponding electronic properties of the metal centers. The strategy presented in this work, that is, designing a system that includes different interactions with hierarchical strengths, can be extended to other related systems and warrants further

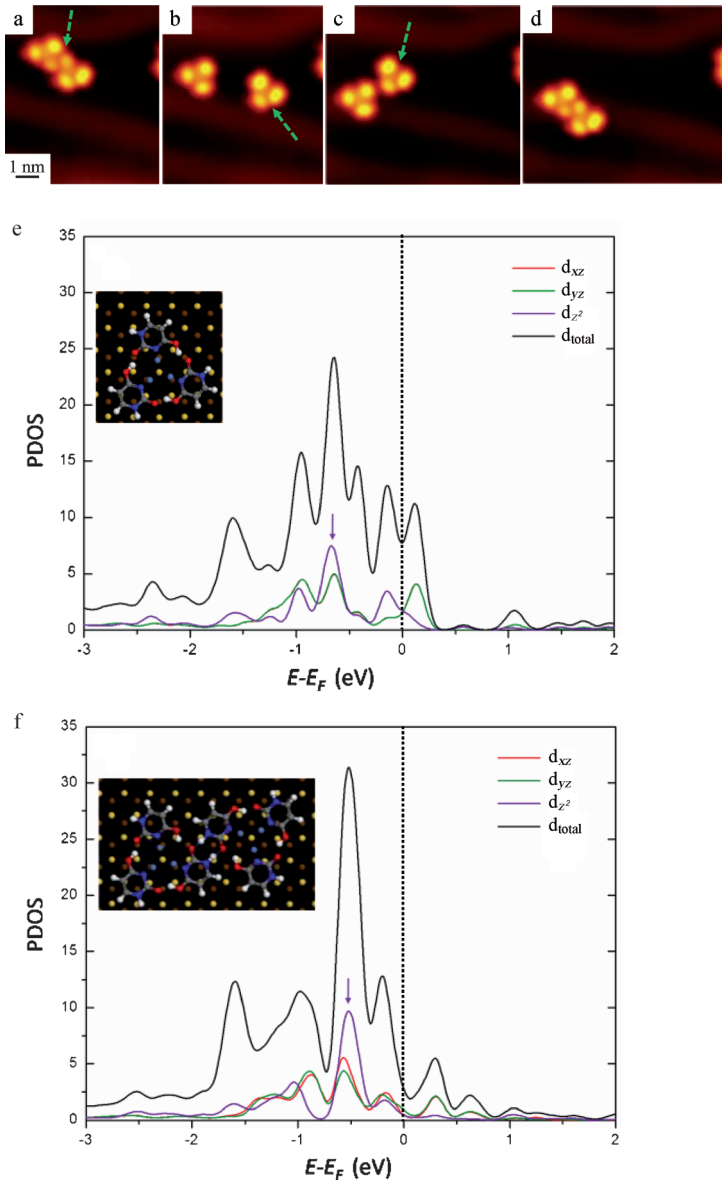

Figure 4. a–d) STM manipulations demonstrating the whole reversible switching process between a parallelogrammic cluster and two triangular clusters. The green arrows indicate the directions of the STM manipulations. e, f) PDOS plots for the d_{xz}, d_{yz}, d_{z^2}, and d_{total} orbitals of the Ni trimer in an isolated triangular cluster and in the same triangle within a parallelogrammic cluster, respectively.

studies on the precise fabrication of artificial molecular nanostructures on surfaces.

Keywords: density functional calculations · metal-organic clusters · scanning tunneling microscopy · surface chemistry

How to cite: *Angew. Chem. Int. Ed.* **2015**, *54*, 6526–6530
Angew. Chem. **2015**, *127*, 6626–6630

[1] L. Gross, K. H. Rieder, F. Moresco, S. M. Stojkovic, A. Gourdon, C. Joachim, *Nat. Mater.* **2005**, *4*, 892–895.
[2] M. Yu, W. Xu, Y. Benjalal, R. Barattin, E. Laegsgaard, I. Stensgaard, M. Hliwa, X. Bouju, A. Gourdon, C. Joachim, T. R. Linderoth, F. Besenbacher, *Nano Res.* **2009**, *2*, 254–259.
[3] J. Liu, C. Li, X. Q. Liu, Y. Lu, F. F. Xiang, X. L. Qiao, Y. X. Cai, Z. P. Wang, S. Q. Liu, L. Wang, *ACS Nano* **2014**, *8*, 12734–12740.
[4] R. Otero, F. Hummelink, F. Sato, S. B. Legoas, P. Thostrup, E. Laegsgaard, I. Stensgaard, D. S. Galvao, F. Besenbacher, *Nat. Mater.* **2004**, *3*, 779–782.
[5] F. Chiaravalloti, L. Gross, K. H. Rieder, S. M. Stojkovic, A. Gourdon, C. Joachim, F. Moresco, *Nat. Mater.* **2007**, *6*, 30–33.
[6] C. Manzano, W. H. Soe, H. S. Wong, F. Ample, A. Gourdon, N. Chandrasekhar, C. Joachim, *Nat. Mater.* **2009**, *8*, 576–579.
[7] L. Grill, K. H. Rieder, F. Moresco, G. Rapenne, S. Stojkovic, X. Bouju, C. Joachim, *Nat. Nanotechnol.* **2007**, *2*, 95–98.
[8] U. G. E. Perera, F. Ample, H. Kersell, Y. Zhang, G. Vives, J. Echeverria, M. Grisolia, G. Rapenne, C. Joachim, S. W. Hla, *Nat. Nanotechnol.* **2013**, *8*, 46–51.
[9] J. K. Gimzewski, C. Joachim, R. R. Schlittler, V. Langlais, H. Tang, I. Johannsen, *Science* **1998**, *281*, 531–533.
[10] V. Simic-Milosevic, J. Meyer, K. Morgenstern, *Angew. Chem. Int. Ed.* **2009**, *48*, 4061–4064; *Angew. Chem.* **2009**, *121*, 4121–4124.
[11] M. Alemani, M. V. Peters, S. Hecht, K. H. Rieder, F. Moresco, L. Grill, *J. Am. Chem. Soc.* **2006**, *128*, 14446–14447.
[12] J. Henzl, M. Mehlhorn, H. Gawronski, K. H. Rieder, K. Morgenstern, *Angew. Chem. Int. Ed.* **2006**, *45*, 603–606; *Angew. Chem.* **2006**, *118*, 617–621.
[13] C. Dri, M. V. Peters, J. Schwarz, S. Hecht, L. Grill, *Nat. Nanotechnol.* **2008**, *3*, 649–653.
[14] W. Auwarter, K. Seufert, F. Bischoff, D. Ecija, S. Vijayaraghavan, S. Joshi, F. Klappenberger, N. Samudrala, J. V. Barth, *Nat. Nanotechnol.* **2012**, *7*, 41–46.
[15] T. Kumagai, F. Hanke, S. Gawinkowski, J. Sharp, K. Kotsis, J. Waluk, M. Persson, L. Grill, *Nat. Chem.* **2014**, *6*, 41–46.
[16] P. Liljeroth, J. Repp, G. Meyer, *Science* **2007**, *317*, 1203–1206.
[17] A. D. Zhao, Q. X. Li, L. Chen, H. J. Xiang, W. H. Wang, S. Pan, B. Wang, X. D. Xiao, J. L. Yang, J. G. Hou, Q. S. Zhu, *Science* **2005**, *309*, 1542–1544.
[18] S. A. Pan, Q. Fu, T. Huang, A. D. Zhao, B. Wang, Y. Luo, J. L. Yang, J. G. Hou, *Proc. Natl. Acad. Sci. USA* **2009**, *106*, 15259–15263.
[19] S. Katano, Y. Kim, M. Hori, M. Trenary, M. Kawai, *Science* **2007**, *316*, 1883–1886.
[20] S. W. Hla, L. Bartels, G. Meyer, K. H. Rieder, *Phys. Rev. Lett.* **2000**, *85*, 2777–2780.
[21] A. Nickel, R. Ohmann, J. Meyer, M. Grisolia, C. Joachim, F. Moresco, G. Cuniberti, *ACS Nano* **2013**, *7*, 191–197.
[22] M. Marschall, J. Reichert, A. Weber-Bargioni, K. Seufert, W. Auwarter, S. Klyatskaya, G. Zoppellaro, M. Ruben, J. V. Barth, *Nat. Chem.* **2010**, *2*, 131–137.
[23] D. Y. Zhong, J. H. Franke, S. K. Podiyanachari, T. Blomker, H. M. Zhang, G. Kehr, G. Erker, H. Fuchs, L. F. Chi, *Science* **2011**, *334*, 213–216.
[24] B. Cirera, Y. Q. Zhang, J. Bjork, S. Klyatskaya, Z. Chen, M. Ruben, J. V. Barth, F. Klappenberger, *Nano Lett.* **2014**, *14*, 1891–1897.
[25] L. Lafferentz, F. Ample, H. Yu, S. Hecht, C. Joachim, L. Grill, *Science* **2009**, *323*, 1193–1197.

[26] T. Lin, G. W. Kuang, W. H. Wang, N. Lin, *ACS Nano* **2014**, *8*, 8310 – 8316.
[27] W. Xu, H. H. Kong, C. Zhang, Q. Sun, H. Gersen, L. Dong, Q. G. Tan, E. Laegsgaard, F. Besenbacher, *Angew. Chem. Int. Ed.* **2013**, *52*, 7442 – 7445; *Angew. Chem.* **2013**, *125*, 7590 – 7593.
[28] L. K. Wang, H. H. Kong, C. Zhang, Q. Sun, L. L. Cai, Q. G. Tan, F. Besenbacher, W. Xu, *ACS Nano* **2014**, *8*, 11799 – 11805.
[29] D. Heim, K. Seufert, W. Auwarter, C. Aurisicchio, C. Fabbro, D. Bonifazi, J. V. Barth, *Nano Lett.* **2010**, *10*, 122 – 128.
[30] J. I. Urgel, D. Ecija, W. Auwarter, J. V. Barth, *Nano Lett.* **2014**, *14*, 1369 – 1373.
[31] C. Zhang, Q. Sun, H. H. Kong, L. K. Wang, Q. G. Tan, W. Xu, *Chem. Commun.* **2014**, *50*, 15924 – 15927.
[32] I. Swart, T. Sonnleitner, J. Niedenfuhr, J. Repp, *Nano Lett.* **2012**, *12*, 1070 – 1074.
[33] P. Liljeroth, I. Swart, S. Paavilainen, J. Repp, G. Meyer, *Nano Lett.* **2010**, *10*, 2475 – 2479.
[34] P. Maksymovych, D. C. Sorescu, K. D. Jordan, J. T. Yates, *Science* **2008**, *322*, 1664 – 1667.
[35] Y. Jiang, Q. Huan, L. Fabris, G. C. Bazan, W. Ho, *Nat. Chem.* **2013**, *5*, 36 – 41.
[36] W. Xu, R. E. A. Kelly, R. Otero, M. Schock, E. Laegsgaard, I. Stensgaard, L. N. Kantorovich, F. Besenbacher, *Small* **2007**, *3*, 2011 – 2014.
[37] Q. Sun, C. Zhang, H. H. Kong, Q. G. Tan, W. Xu, *Chem. Commun.* **2014**, *50*, 11825 – 11828.
[38] H. H. Kong, L. K. Wang, Q. G. Tan, C. Zhang, Q. Sun, W. Xu, *Chem. Commun.* **2014**, *50*, 3242 – 3244.
[39] H. H. Kong, Q. Sun, L. K. Wang, Q. G. Tan, C. Zhang, K. Sheng, W. Xu, *ACS Nano* **2014**, *8*, 1804 – 1808.
[40] D. Y. Zhong, T. Blomker, C. Mück-Lichtenfeld, H. M. Zhang, G. Kehr, G. Erker, H. Fuchs, L. F. Chi, *Small* **2014**, *10*, 265 – 270.
[41] A. C. Papageorgiou, S. Fischer, J. Reichert, K. Diller, F. Blobner, F. Klappenberger, F. Allegretti, A. P. Seitsonen, J. V. Barth, *ACS Nano* **2012**, *6*, 2477 – 2486.
[42] V. Iancu, A. Deshpande, S. W. Hla, *Phys. Rev. Lett.* **2006**, *97*, 266603.

Received: February 23, 2015
Published online: April 15, 2015

